Combining Transversal and Longitudinal Registration in IVUS Studies

G.D. Maso Talou[1,2], P.J. Blanco[1,2], I. Larrabide[3], C. Guedes Bezerra[4,5], P.A. Lemos[4,5], and R.A. Feijóo[1,2]

[1] Laboratório Nacional de Computação Científica, LNCC-MCTI, Av. Getúlio Vargas 333, 25651-075 Petrópolis, Brazil
[2] Instituto Nacional de Ciência e Tecnologia em Medicina Assistida por Computação Científica, INCT-MACC, Petrópolis, Brazil
[3] Comisión Nacional de Investigaciones Científicas y Técnicas, Pladema - CONICET, UNICEN, Tandil, Argentina
[4] Instituto do Coração (InCor), São Paulo, SP, 05403-904, Brazil
[5] Universidad de São Paulo, Faculdade de Medicina, São Paulo, SP, 05403-904, Brazil

Abstract. Intravascular ultrasound (IVUS) is a widely used imaging technique for atherosclerotic plaque assessment, interventionist guidance, stent deploy visualization and, lately, as tissue characterization tool. Some IVUS applications solve the problem of transducer motion by gating a particular phase of the study while others, such as elastography or spatio-temporal vessel reconstruction, combine image data from different cardiac phases, for which the gating solution is not enough. In the latter, it is mandatory for the structures in different cardiac phases to be aligned (cross-sectional registration) and in the correct position along the vessel axis (longitudinal registration). In this paper, a novel method for transversal and longitudinal registration is presented, which minimizes the correlation of the structures between images in a local set of frames. To assess the performance of this method, frames immediately after carina bifurcation were marked at different cardiac phases and the error between registrations was measured. The results shown a longitudinal registration error of 0.3827 ± 0.8250 frames.

Keywords: IVUS, transversal registration, longitudinal registration, cardiac phases.

1 Introduction

Intravascular ultrasound (IVUS) is an imaging technique widely used for atherosclerotic plaque assessment. During its acquisition, the heart contraction imprints a motion pattern on the transducer and the vessel (referred to as cardiac dynamic component), misleading the identification of frame spatial location at non-diastolic phases. The transducer motion can be decomposed in two spatial components, the transversal motion and the longitudinal motion. The former produces a translation and rotation of the structures from one image to the

N. Navab et al. (Eds.): MICCAI 2015, Part II, LNCS 9350, pp. 346–353, 2015.
DOI: 10.1007/978-3-319-24571-3_42

next, while the latter produces a proximal/distal displacement additional to the pullback [3,4].

The transversal motion component has been widely treated by rigid [13,8,14,9,6,16,15,5] and non-rigid [2,7] registration approaches. In contrast, the longitudinal motion component is usually neglected even though [3] reported an average axial displacement of 1.5 ± 0.8 mm in 0.016 mm interframe acquisitions. Due to the catheter migration, the transversal region observed in systolic phases is much more proximal than expected (mean offset of 93.75 frames). As a consequence the wall strain estimation from the IVUS images along the cardiac phases is not necessarily valid. In [12] a method for rigid longitudinal motion is proposed which aligns each cardiac phase against the diastolic phase of the study. A more complete scheme is proposed in [10] performing longitudinal prior transversal registration of two cardiac phases of the study.

In our work, we present a method to treat both motion components involved in the transducer displacement after the gating process. The goal here is to improve the registration accuracy by identifying both motion components in a fully coupled manner. To measure the accuracy of the methods, bifurcations carina locations are identified manually across different cardiac phases of in-vivo studies. After the registration process, it is expected that bifurcations are registered at the same longitudinal position. Then, the difference in the spatial position is computed as the longitudinal registration error.

2 Methodology

2.1 IVUS Pre-processing

A region of interest (ROI) for the k-th frame $J_k(x, y)$ of the original IVUS sequence, is defined as the non-zero values of the binary mask $M_k(x, y)$ with the same size of the IVUS frame. Similarly, we define $M_{\mathrm{DR}}(x, y)$ and $M^k_{\mathrm{GW}}(x, y)$ as the binary masks associated to the down-ring and the guidewire artifacts regions. Then, the image mask in the k-th frame is defined as $M_k = \neg(M_{\mathrm{DR}} \vee M^k_{\mathrm{GW}})$ where $\neg$ and $\vee$ stand for NOT and OR boolean operators, respectively. The ROI described by M_k is artifact free and will be used to assess similarity between vessel structures of two different IVUS frames. $M_{\mathrm{DR}}(x, y)$ and $M^k_{\mathrm{GW}}(x, y)$ can be obtained semi-automatically as described in [11].

2.2 Cross-Sectional Registration

Let us define a similarity function, c, that measures alignment of structures between two frames. For the given IVUS frames J_n and J_m and the corresponding ROIs M_n and M_m, we define a common ROI as $M_{n,m} = M_n \wedge M_m$ where $\wedge$ is the AND boolean operator. Pixel set $\mathscr{R}^{n,m} = \{(x, y),\, M_{n,m}(x, y) = 1\}$ is used to construct a normalized cross-correlation function that compares pixels in $\mathscr{R}^{n,m}$ as follows

$$c(J_n, J_m)|_{\mathscr{R}} = \frac{\sum_{(x,y)\in\mathscr{R}^{n,m}} (J_n(x, y) - \mu_n)\,(J_m(x, y) - \mu_m)}{\sigma_n\ \sigma_m} \tag{1}$$

where μ_n and σ_n are the mean and standard deviation of the $\mathscr{R}^{n,m}$ values of frame J_n. Cross-correlation provides a fair comparison of the vessel structures due to the correlation between noise pattern and tissue micro-structure [1].

Thus, we search for the rigid motion that maximizes the similarity function c between the two frames. The rigid motion, called Ξ, is described by the horizontal and vertical displacements, τ_x and τ_y, and a rotation around the center of the frame θ. Then, Ξ that maps J_m onto J_n, is defined as

$$\Xi_m^n = \arg\max_{\Xi^* \in \mathscr{U}} \mathscr{F}(J_n, J_m, \Xi^*) = \arg\max_{\Xi^* \in \mathscr{U}} c(J_n, J_m(x(\Xi^*), y(\Xi^*)))|_{\mathscr{R}} \quad (2)$$

where $\mathscr{U}$ is the space of admissible rigid motions of the transducer and $J_m(x(\Xi^*), y(\Xi^*))$ is the frame J_m after applying the rigid motion Ξ^* through which the coordinate (x, y) is displaced. Because of the acquisition sampling, the space $\mathscr{U}$ is discrete and translations and rotations only make sense for multiples of one pixel and $\frac{2\pi}{256}$ radians, respectively. Also, the transducer is confined to the lumen restricting horizontal and vertical displacements. Thus, we characterize $\mathscr{U} = \{\Xi = (\tau_x, \tau_y, \theta)\}$, where $\theta = i\frac{\pi}{128}, i = 0, \ldots, 255$, $\tau_x \in [\tau_x^{\mathrm{m}}, \tau_x^{\mathrm{M}}] \subset \mathbb{Z}$ and $\tau_y \in [\tau_y^{\mathrm{m}}, \tau_y^{\mathrm{M}}] \subset \mathbb{Z}$ being $\tau_{(\cdot)}^{\mathrm{M}}$ and $\tau_{(\cdot)}^{\mathrm{m}}$ the maximum and minimum admissible displacement in $(\cdot)$ direction.

Equation 2 involves the maximization of a not necessarily convex functional. Then, we propose a novel heuristic approach called multi-seed gradient ascend (MSGA) method to account for the non-convexity of the problem. Here, multiple initializations are used to ascend and the instance that reaches maximum functional cost value is considered to be the solution. A suitable trade-off between accuracy and performance is found for an initialization with 5 equidistant seeds.

2.3 Longitudinal Registration

Longitudinal registration is performed between volumes of different cardiac phases. For this, IVUS studies are recorded synchronously with the patient ECG. Then, a specialist indicates in the ECG the R-wave peak moment identifying the first cardiac phase volume. Other P cardiac phase volumes are extracted by picking the $1, \ldots, P$ next frames of the original IVUS volume. Although the images within each set are ordered longitudinally, displacements between frames may not necessarily be homogeneous because of the large variability in the transducer motion throughout the cardiac cycle. Particularly, a diastolic phase before cardiac contraction, referred to as *steady phase*, is assumed to feature homogeneous displacement field as a result of the reduced cardiac motion. Then, from the $\mathscr{I}_i$, $i = 1, \ldots, P$ cardiac phases, we define the steady phase $\mathscr{I}_{\mathrm{st}}$ as

$$\mathscr{I}_{\mathrm{st}} = \arg\min_{i=1,\ldots,P} \mathscr{P}_{\mathrm{motion}}(\mathscr{I}_i) = \arg\min_{i=1,\ldots,P} \left\{ -\frac{1}{N_i} \sum_{j=1}^{N_i} \sum_{y=1}^{H} \sum_{x=1}^{W} \left| \nabla I_j^i(x, y) \right| \right\} \quad (3)$$

where I_j^i denotes the j-th study frame in the i-th phase, N_i is the number of frames for that i-th cardiac phase, and H and W are the study frame dimensions and ∇ is the gradient operator. Steady phase frames will be denoted as I_j^{st}.

With motionless assumption at the steady phase, the longitudinal location of its frames along the catheter is characterized as $r(I_j^{\mathrm{st}}) = r_0 + \frac{j\, v_p}{f_s}$ where I_j^{st} is the j-th study frame in the phase $\mathscr{I}_{\mathrm{st}}$, r_0 is the transducer initial position over the longitudinal axis, v_p is the pullback velocity in $mm \cdot s^{-1}$ and f_s is the acquisition framerate in $frame \cdot s^{-1}$.

The steady phase $\mathscr{I}_{\mathrm{st}}$, and the known spatial location of the corresponding frames I_j^{st}, $j = 1, \ldots, N_{\mathrm{st}}$, is used to perform a non-linear longitudinal registration of the remaining phases, hereafter referred to as *non-steady phases*. The registration process consists in assessing the similarity of each non-steady phase frame against the steady phase frames. The most similar steady phase is used to place the non-steady one. For the i-th cardiac phase, the degree of similarity between j-th frame I_j^i and I_k^{st}, $k = 1, \ldots, N_{\mathrm{st}}$, is measured through a neighborhood correlation defined as follows

$$c_w(I_j^i, I_k^{\mathrm{st}}) = \frac{\sum_{d=-w}^{w} \phi(d,\sigma_{\mathrm{G}})\, c(I_{j+d}^i, I_{k+d}^{\mathrm{st}})|_{\mathscr{R}}}{\sum_{d=-w}^{w} \phi(d,\sigma_{\mathrm{G}})}, \tag{4}$$

where w is the frame neighborhood width and ϕ is a Gaussian weight function with σ_{G} standard deviation. The parameter w is defined as $w(\sigma, T) = \left\lfloor \sigma(-2\ln(T))^{\frac{1}{2}} \right\rfloor$ to neglect the contributions from frames with weights that are smaller than $T\ \phi(0, \sigma_{\mathrm{G}})$ (with $T = 10^{-1}$). The parameter σ_{G} should be small enough to be representative of the local structures and large enough to incorporate information about the longitudinal structure to achieve robustness (Section 3.2). Finally, the position in space of the frame I_j^i, which belongs to a *non-steady phase*, i.e. $i \neq \mathrm{st}$, is defined as $r(I_j^i) = r(I_m^{\mathrm{st}})$ where $m = \underset{k=1,\ldots,N_{\mathrm{st}}}{\arg\max}\, c_w(I_j^i, I_k^{\mathrm{st}})$. A formal definition for the set of frames located at the n-th frame position of the steady phase, is given by $\mathscr{X}_n = \{I_j^i;\, r(I_j^i) = r(I_n^{\mathrm{st}}),\, j = 1, \ldots, N_i, i = 1, \ldots, P\}$.

The estimated transducer motion (Figure 1) resembles the motion pattern experimentally observed in medical practice. Specifically, the pseudo-periodic proximal-distal oscillations and their amplitudes obtained here, are within the ranges reported experimentally in [3].

2.4 Coupling Transversal and Longitudinal Registration

Cross-sectional registration is performed prior the comparison presented in (4). In that manner, the position in space of the frame I_j^i, which belongs to a *non-steady phase* and the applied transversal rigid motion Ξ_j^i to that frame are defined as $r(I_j^i(x(\Xi_j^i), y(\Xi_j^i))) = r(I_m^{\mathrm{st}})$, where

$$m = \underset{k=1,\ldots,N_{\mathrm{st}}}{\arg\max}\, c_w(I_j^i(x(\Xi_j^i), y(\Xi_j^i)), I_k^{\mathrm{st}}) \tag{5}$$

and

$$\Xi_j^i = \underset{\Xi^* \in \mathscr{U}}{\arg\max} \sum_{d=-w}^{w} \mathscr{F}(I_{k+d}^{\mathrm{st}}, I_{j+d}^i, \Xi^*). \tag{6}$$

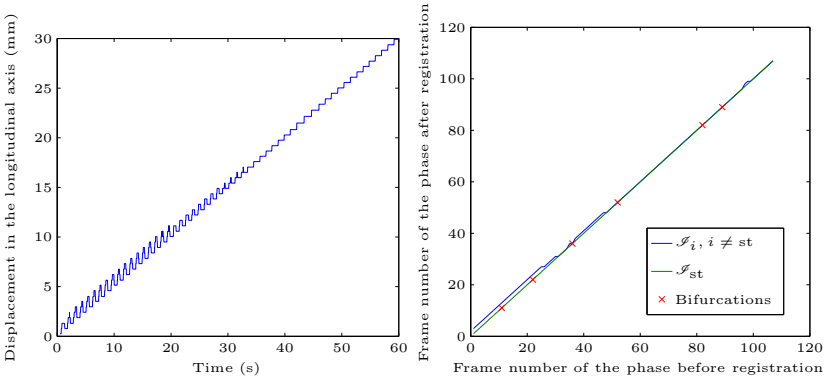

Fig. 1. Longitudinal registration process in-vivo using $\sigma_{\text{G}} = 0.4$: (Left) Transducer longitudinal displacement; (Right) Registration of a non-steady cardiac phase against $\mathscr{I}_{\text{st}}$.

Note that the transversal registration performed in (6) is now coupled with the longitudinal registration due to (5). Although, this implementation models a more suitable scheme for the longitudinal comparison due to the alignment of the structures, it also increases the computational cost. Finally, the aligned set of frames located at the n-th frame position of the steady phase, is given by $\mathscr{X}_n^{\text{C}} = \{I_j^i(x(\Xi_j^i), y(\Xi_j^i));\ r(I_j^i(x(\Xi_j^i), y(\Xi_j^i))) = r(I_n^{\text{st}}),\ j = 1, \ldots, N_i, i = 1, \ldots, P\}$.

3 Results and Discussion

3.1 IVUS Data

The IVUS studies were acquired with the Atlantis$^{\text{TM}}$SR Pro Imaging Catheter at 40 MHz synchronized with an ECG signal and connected to an iLab$^{\text{TM}}$ Ultrasound Imaging System (both by Boston Scientific Corporation, Natick, MA, USA), at the Heart Institute (InCor), University of São Paulo Medical School and Sírio-Libanês Hospital, São Paulo, Brazil. The procedure was performed during a diagnostic or therapeutic percutaneous coronary procedure. Vessels were imaged using automated pullback at 0.5 mm/s. Overall, 30 IVUS studies with synchronized ECG signal were performed on different patients.

3.2 Validation Using Bifurcation Sites

Bifurcation sites, more precisely the first frame of anastomosis, were used as landmark points to assess the longitudinal misalignment between two phase image volumes. Then, we define longitudinal registration error as $\varepsilon^k = \frac{1}{NB} \sum_{j=1}^{NB} |B^{\text{st}}(j) - B^k(j)|$ where NB is the number of bifurcations in the study, $B^k(j)$ is the frame at the j-th bifurcation in the k-th cardiac phase.

Table 1 presents ε^k for different values of σ_{G} which determines the frames neighborhood (w). Values for σ_{G} where chosen such as w differs by 1 between

Table 1. Mean ($E(\varepsilon^k)$) and standard deviation ($s(\varepsilon^k)$) of the longitudinal registration error in frames for different values of σ_G for 30 IVUS studies.

w	0	1	2	3	4
σ_G	0.4	0.8	1.2	1.6	2.0
$E(\varepsilon^k)) \pm s(\varepsilon^k)$	0.383 ± 0.825	0.506 ± 1.48	0.630 ± 2.009	0.605 ± 1.991	0.470 ± 1.532

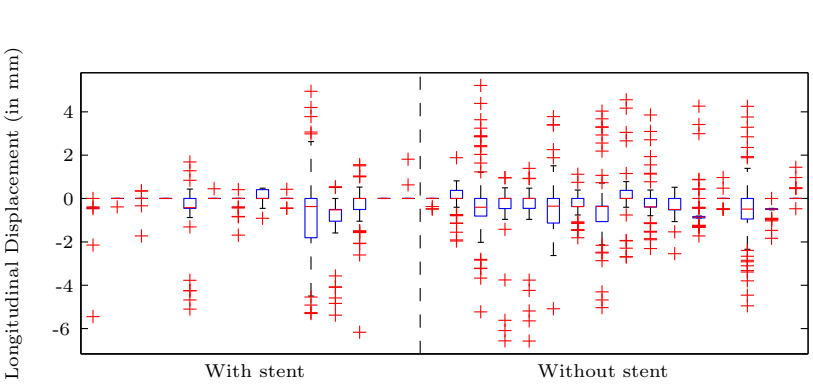

Fig. 2. Box plot presenting the transducer longitudinal displacements at each heartbeat for all the studies, dividing them as patients with or without stent deployment.

comparisons, evidencing the neighbor contribution. The registration process rendered the lowest discrepancy against the specialist identification for $\sigma_G = 0.4$ (error of 0.3827 ± 0.8250 frames). This means that the usage of adjacent frames data does not improve the registration and this is because of two factors: i) the presence of adventitia and luminal areas with decorrelated noise within the ROI; ii) the variation of the motion pattern in successive heartbeats. In the following sections σ_G is fixed to 0.4.

3.3 Correlation between Longitudinal Motion and Stent Deployment

IVUS studies were divided in 2 groups of cases: studies with stent (N=14) and without stent (N=16). Using the longitudinal displacement applied for longitudinal registration of the systolic and diastolic phase (phases with highest and lowest values of $\mathscr{P}_{\text{motion}}$) of each study, we measure the amplitude of the transducer migration during the cardiac cycle. In Figure 2 a reduction of the longitudinal displacements amplitude can be noticed for cases with stent deployment. A longitudinal displacement of 0.283 ± 0.739 mm and 0.519 ± 0.785 (absolute value of displacements) for cases with and without stent deployment is observed, respectively. These results confirm the previous findings reported in [3].

For further analysis, the longitudinal displacement was calculated in an artery before and after stent deployment (Figure 3). As result, the method shows reproducibility, i.e., it delivers a close displacement pattern at the stent distal

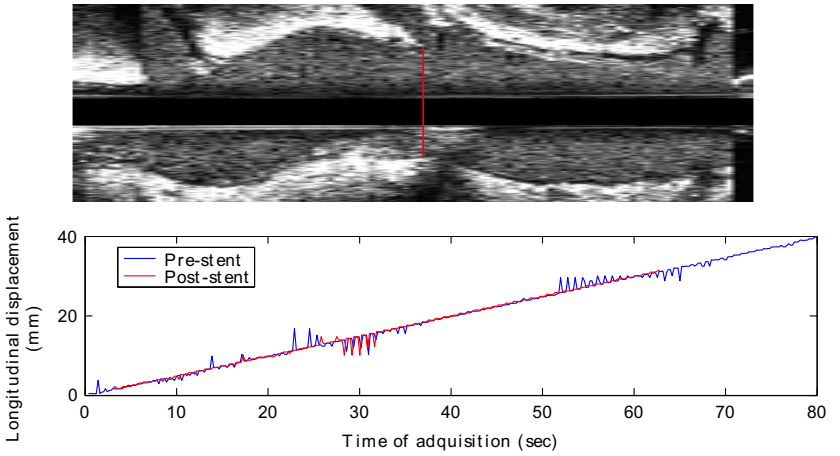

Fig. 3. Estimation of the transducer longitudinal displacement before and after stent deployment: (top) longitudinal view at $\mathscr{I}_{\text{st}}$ phase (left is the distal position); (bottom) Transducer longitudinal displacement. The red line marks the distal point of the stent.

positions in both cases (before and after stenting). Also, a complete attenuation of the longitudinal displacement upstream the stent area is observed. Hence, downstream displacements are slightly larger after the stenting procedure.

4 Conclusions

A novel method for longitudinal and transversal registration of IVUS studies was presented. It is concluded that the optimal longitudinal registration is performed when only local cross sectional data are used. Comparisons against a specialist shows an error of 0.3827 ± 0.8250 frames at the bifurcation sites. The inclusion of neighbor frames at the registration deteriorates the block matching with a ROI of the full image (excluding image artifacts). Further works, may include the use of different ROIs excluding the adventitia and lumen areas where the data is not reliable for matching the vessel wall structures. Performance issues must be further explored, although the present strategy allows a parallelization at frame comparison level that is well suited for GP-GPU implementations.

The motion estimated by the longitudinal registration has also been used to study the association of the transducer longitudinal displacement and stenting. Remarkably, the proposed method estimates larger motion in non-stented vessels, while smaller displacements are observed in stented vessels confirming previous findings. Future work will include larger patient populations.

Acknowledgements. This research was partially supported by the Brazilian agencies CNPq, FAPERJ and CAPES. The support of these agencies is gratefully acknowledged. Also, the authors would like to thank the anonymous reviewers for their valuable comments and suggestions to improve the quality of the paper.

References

1. Abbott, J.G., Thurstone, F.L.: Acoustic speckle: Theory and experimental analysis. Ultrason. Imag. 324(4), 303–324 (1979)
2. Amores, J., Radeva, P.: Retrieval of IVUS images using contextual information and elastic matching. Int. J. Intell. Syst. 20(5), 541–559 (2005)
3. Arbab-Zadeh, A., DeMaria, A.N., Penny, W.F., Russo, R.J., Kimura, B.J., Bhargava, V.: Axial movement of the intravascular ultrasound probe during the cardiac cycle: implications for three-dimensional reconstruction and measurements of coronary dimensions. Am. Heart J. 138(5 Pt 1), 865–872 (1999)
4. Bruining, N., von Birgelen, C., de Feyter, P.J., Ligthart, J., Li, W., Serruys, P.W., Roelandt, J.R.: Ecg-gated versus nongated three-dimensional intracoronary ultrasound analysis: implications for volumetric measurements. Cathet. Cardiovasc. Diagn. 43(3), 254–260 (1998)
5. Danilouchkine, M.G., Mastik, F., van der Steen, A.F.: Improving IVUS palpography by incorporation of motion compensation based on block matching and optical flow. IEEE Trans. Ultrason. Ferroelectrics Freq. Contr. 55(11), 2392–2404 (2008)
6. Hernandez-Sabate, A., Gil, D., Fernandez-Nofrerias, E., Radeva, P., Marti, E.: Approaching artery rigid dynamics in IVUS. IEEE Trans. Med. Imag. 28(11), 1670–1680 (2009)
7. Katouzian, A., Karamalis, A., Lisauskas, J., Eslami, A., Navab, N.: IVUS-histology image registration. In: Dawant, B.M., Christensen, G.E., Fitzpatrick, J.M., Rueckert, D. (eds.) WBIR 2012. LNCS, vol. 7359, pp. 141–149. Springer, Heidelberg (2012)
8. Leung, K.Y.E., Baldewsing, R., Mastik, F., Schaar, J.A., Gisolf, A., van der Steen, A.F.W.: Motion compensation for intravascular ultrasound palpography. IEEE Trans. Ultrason. Ferroelectrics Freq. Contr. 53(7), 1269–1280 (2006)
9. Liang, Y., Zhu, H., Friedman, M.H.: Estimation of the transverse strain tensor in the arterial wall using IVUS image registration. Ultrasound Med. Biol. 34(11), 1832–1845 (2008)
10. Liang, Y., Zhu, H., Gehrig, T., Friedman, M.H.: Measurement of the transverse strain tensor in the coronary arterial wall from clinical intravascular ultrasound images. J. Biomech. 41(14), 2906–2911 (2008)
11. Maso Talou, G.D.: IVUS images segmentation driven by active contours and spaciotemporal reconstruction of the coronary vessels aided by angiographies. Master's thesis, National Laboratory for Scientific Computing, Petrópolis, Brazil (2013)
12. Matsumoto, M.M.S., Lemos, P.A., Furuie, S.S.: Ivus coronary volume alignment for distinct phases. In: SPIE Medical Imaging, p. 72650X. International Society for Optics and Photonics (2009)
13. Mita, H., Kanai, H., Koiwa, Y.: Cross-sectional elastic imaging of arterial wall using intravascular ultrasonography. Jpn. J. Appl. Phys. 40(7), 4753–4762 (2001)
14. Oakeson, K.D., Zhu, H., Friedman, M.H.: Quantification of cross-sectional artery wall motion with ivus image registration. In: Medical Imaging 2004, pp. 119–130. International Society for Optics and Photonics (2004)
15. Rosales, M., Radeva, P., Rodriguez-Leor, O., Gil, D.: Modelling of image-catheter motion for 3-D IVUS. Medical Image Analysis 13(1), 91–104 (2009)
16. Zheng, S., Jianjian, W.: Compensation of in-plane rigid motion for in vivo intracoronary ultrasound image sequence. Comput. Biol. Med. 43(9), 1077–1085 (2013)